Lambda-Point Measurements of $\eta\rho_n$ for Pure He^4 and for Three He^3-He^4 Mixtures

R. W. H. Webeler and G. Allen
Lewis Research Center, National Aeronautics and Space Administration, Cleveland, Ohio 44135
(Received 7 September 1971)

Torsional crystal measurements of $\eta\rho_n$ have been made for pure He^4 and for three He^3-He^4 mixtures ($x_3 = 0.005$, 0.047, and 0.100) over temperature intervals which included their respective λ points. The precision of the measurements for the mixtures was greater than that of any previous λ-point $\eta\rho_n$ measurements. Doubly reduced plots of $\eta\rho_n$ versus T showed a slight but definite tendency for such curves to rotate clockwise about the (1, 1) point with increasing x_3 up to about 0.05. Values of η were derived from the measurements by computing ρ_n as a function of T^*. For each mixture, both η and $d\eta/dT$ were continuous across $T_\lambda(x_3)$. No tendency was manifest for such curves to develop discontinuities as x_3 decreased. It was, therefore, inferred that both η and $d\eta/dT$ of pure He^4 are continuous across $T_\lambda(0)$. A further result obtained here is that, up to $x_3 = 0.100$, the λ viscosity of the mixture $\eta_\lambda(x_3)$ bears a linear relationship to the λ temperature of $T_\lambda(x_3)$.

I. INTRODUCTION

Although measurements of the viscosity of liquid He^4 have been carried out for more than 60 years over a wide range of experimental conditions, good reasons for further investigations still remain. First of all, there is a wide divergence among published viscosity values η below 1.3 K.[1] Second, while there is much better agreement near 2 K, the question concerning the continuity of η and/or $d\eta/dT$ across T_λ remains unanswered and the existing data are rather sparse near T_λ.

One experimental problem in obtaining viscosity data in the neighborhood of T_λ is the determination of the temperature of the sample fluid. For $T < T_\lambda$, the very high heat-transport properties of liquid He^4 makes it an ideal heat-reservoir material. But very close to T_λ, its heat-transport properties rapidly decrease and, above T_λ, they are poor. If the sample fluid and bath reservoir are both He^4, then they will both pass through their λ points at about the same time. This will destroy the isothermal environment of the sample fluid, making it difficult to obtain a precise unambiguous temperature.

To overcome this difficulty, the λ point of the sample fluid can be depressed below that of the reservoir. Then the reservoir maintains excellent heat-transport properties on both sides of the λ point of the sample fluid. This can be accomplished by keeping the sample fluid at a higher pressure than the bath, but this method can result in other difficulties.[2] Another way to depress the λ point is to add some He^3 to the sample fluid. This method, which was used in the present investigation, enables highly reproducible measurements to be made on the sample fluid in the immediate vicinity of and across its λ point. However, the data are then measurements of the He^3-He^4 mixtures, rather than of pure He^4.

This last point is not a disadvantage, of course. In the first place, such data on the mixtures are of interest in themselves. The only previously published viscosity values of He^3-He^4 mixtures in temperature intervals which include their respective λ points are the rather sparse data of Dash and Taylor.[3] Staas *et al.*[4] reported viscosity values as a function of temperature for He^3-He^4 mixtures over a wide range of concentrations of He^3, but all of these latter measurements are below the λ points of the respective mixtures $T_\lambda(x_3)$. Their absolute values also appear to be about 20% too low. A fairly comprehensive list of references to previous work can be found in Ref. 5. In the second place, the present measurements turned out to be so precise that some inferences about pure He^4 could be obtained by extrapolation from the dilute mixtures. These inferences, which concern the continuity of η and $d\eta/dT$ across $T_\lambda(0)$, could not be made from the available data for pure He^4.

In this investigation, using the torsional crystal technique, measurements were made of $\eta\rho_n$ as a function of temperature for pure He^4 and for He^3-He^4 mixtures containing three different concentrations of He^3: $x_3 = 0.005$, 0.047, and 0.1005. Here, ρ_n is the normal density of the mixture and x_3 is the mole fraction of He^3 atoms in the mixture.

After examining some alternatives, it was decided that a very useful way to compare results for different concentrations of He^3 was to make doubly reduced plots of the data. In these plots, not only the temperature but also the ordinates are expressed as multiples of the λ-point values. On such a plot, the λ transition is always located at (1, 1). The use of such plots for the mixtures and pure He^4 in the present investigation enabled

us to determine the (1, 1) point more accurately than had been done in Ref. 6. In fact, we were able to determine a temperature correction for data given in Ref. 6.

Furthermore, the availability of accurate values of the normal density of pure He^4 enabled the viscosity to be derived from our measured values of $n\rho_n$. An examination of the η-versus-T^* plots established the inference that there is no discontinuity in either η or $d\eta/dT$ across $T_\lambda(0)$ for pure He^4.

II. EXPERIMENTAL PROCEDURE AND APPARATUS

A piezoelectric cylindrical quartz crystal was immersed in the liquid of interest and driven in a torsional mode of vibration at its resonant frequency of 11 kHz. The logarithmic decrements were then determined as a function of temperature by measuring the crystal resistance at resonance. This method of measuring the viscosity was first used by Welber and Quimby.[7] As a result of a number of refinements in the apparatus, the sensititivy and precision of the method have been greatly improved.[5]

A silver crystal holder served as a support for four pure-silver electrode quadrants that surround, but do not contact, the crystal (Fig. 1). The crystal was 0.53 cm in diameter by 17.7 cm long and was supported by two nylon threads at its central displacement node. The space between the electrode quadrants and the crystal surface (about 0.5 mm) was filled by the mixture of interest, and it was this portion of the total amount of fluid (about 0.75 mole) in the copper sample chamber which provided the measured decrement.

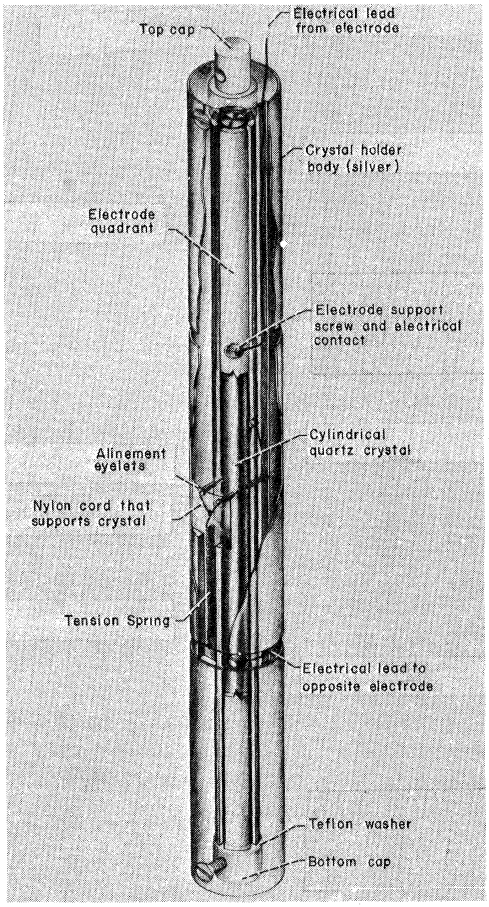

FIG. 1. Torsional crystal suspension system prior to placement in sample chamber of Fig. 2.

The crystal resistance was measured by capacitance coupling to the electrode quadrants, which thereby eliminated the need for a mechanical contact. These quadrants were connected to one arm of a modified Schering capacitance bridge by small electrical wires running inside a capillary tube from the sample chamber to room temperature. A PAR two-phase lock-in amplifier was used to detect the null bridge balance for small driving voltages (4–9 mV) across the crystal at the crystal resonant frequency.

The low-temperature apparatus used in this investigation (see Fig. 2) was originally designed for measurements near 0.1 K rather than specifically for measurements near 2.0 K. However, some minor modifications made it suitable for the λ-point measurements for which it was used. By drilling a number of holes in the bottom of the brass chamber of the apparatus, the middle chamber (which surrounds the sample chamber), could be filled with liquid He^4 from the bath reservoir. Thus the liquid He^4 in the middle chamber was in contact with the copper sample chamber and served as a heat exchanger between the reservoir and the sample chamber. In this way, the temperature of the sample chamber was regulated by the temperature of the liquid He^4 in the reservoir. The temperature of the reservoir was controlled by a Texas Instruments Bourdon tube pressure gauge (TIBTPG), a Texas Instruments pressure controller (TIPC), two pumping systems for the reservoir, and an auxiliary He^4 gas supply. The latter was bled into the reservoir system at a rate determined by the TIPC. The TIBTPG sensed the vapor pressure of the liquid He^4 in the middle chamber with a sensitivity better than one part in ten thousand. Temperature changes less than 0.1 mK could be detected.

The temperature controller functioned as follows: The TIBTPG was set to provide a zero error signal at a given vapor pressure corresponding to the temperature at which data were to be taken. If the vapor pressure in the middle chamber deviated from the chosen setting, the TIBTPG produced an error signal which was sensed by the servomechanism in the TIPC and accordingly adjusted the flow of He^4 gas into the reservoir system and pumping lines. This method of sensing the vapor pressure of the middle chamber and using the flow of He^4 gas into the reservoir system to change the tempera-

ture of the reservoir will not work above the λ-point temperature of the bath. On the other hand, it works very well near but below the bath λ transition.

It was necessary to have a primary pumping system in addition to the pumping system required in conjunction with the TIPC. When both pumping systems and the temperature control system were operating properly, no temperature oscillations were detectable. The electrical resistance of the crystal varied rapidly with temperature just below $T_\lambda(x_3)$ due to the rapidly changing values of $\eta\rho_n$. In fact, for dilute mixtures of He^3 in He^4, a small change in its temperature near but below $T_\lambda(x_3)$ was accompanied by an order-of-magnitude greater change in $\eta\rho_n$. Crystal resistance changes of a few parts in 30 000 could be detected, so that such measurements provided another more sensitive means of checking on the temperature stability of the temperature control system to supplement the measurement of just the temperature or the vapor pressure.

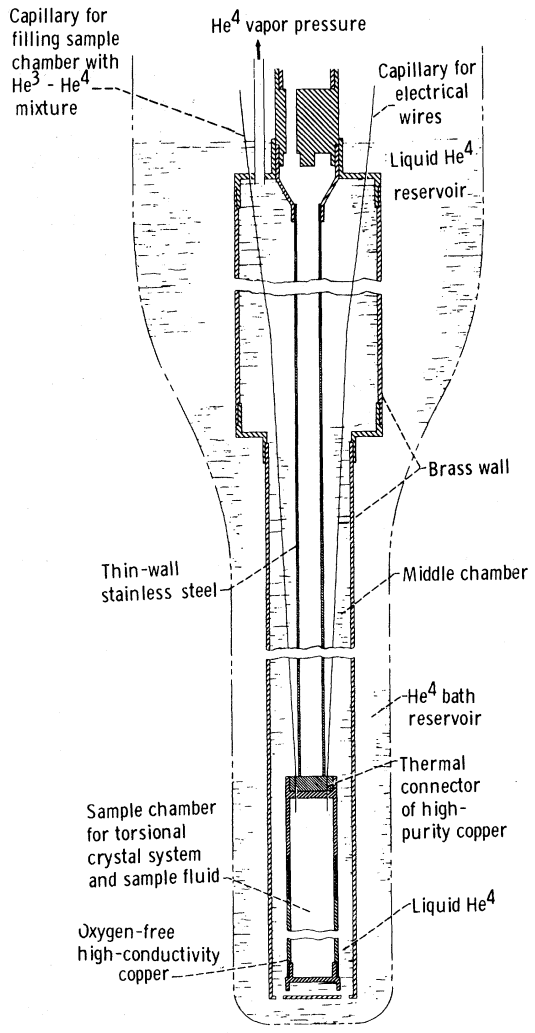

FIG. 2. Schematic of low-temperature apparatus.

The sample temperature was determined both from resistance thermometer measurements and vapor pressure measurements of the liquid He^4 in the chamber. The useful thermometers in the sample chamber consisted of four nominal 10-Ω 0.1-W Allen-Bradley carbon composition resistors. These thermometers were mounted in the sample chamber in a previous experiment and so were retained even though their dR/dT was not optimum near 2 K. These resistors were wired electrically in parallel and calibrated by means of vapor-pressure measurements from liquid He^4 in the middle chamber. A fused quartz Bourdon tube with a range of 0.0–253 Torr was in the TIBTPG which was used to measure the vapor pressure. The absolute temperature could only be determined to within 2 mK, but changes within 0.1 mK were detectable.

If the middle chamber contained liquid He II, it was found that the TIBTPG determined the temperature of the sample chamber with better precision than the nominal 10-Ω Allen-Bradley resistance thermometers. (Temperature changes could be determined with a precision of 0.1 mK using resistance thermometers.) However, this was not true when the middle chamber contained He I. At and above the λ point of the He^4 in the middle chamber and reservoir, only the resistance thermometers were useful in determining sample chamber temperature.

Since the absolute temperature of the sample could not be determined more accurately than to 1–2 mK, the measured temperature could not be used to locate the λ transition for pure He^4 or any of the mixtures with sufficient accuracy. The experimental λ point for any particular mixture was chosen by carefully locating the temperature at which a discontinuity in the slope of the $\eta\rho_n$ occurred. This method of locating the λ point was not used for pure He^4 because of the large scatter of the pure-He^4 data. For pure He^4, the λ point was located by adding a correction to the very precisely determined experimental λ temperature for the $\frac{1}{2}\%$ mixture. The experimental $T_\lambda(0)$ used was $T_\lambda(0.005) + |\Delta T|$, where ΔT is the amount by which the λ point of pure He^4 differs from that of the 0.005-mole fraction of He^3. To sufficient accuracy this decrease follows the two-thirds power of x_4.[3] The composition of the mixtures was determined by first introducing a measured pressure of He^3 gas into an evacuated tank, and then introducing pure-He^4 gas from a high-pressure source until the desired composition resulted (assuming ideal-gas behavior). The accuracy with which the composi-

tion was prepared was limited only by the accuracy with which the pressures could be determined from the TIBTPG. This was better than 2% for the 0.005-mole-fraction mixture which was the least accurate. However, this, in general, was not a true indication of the accuracy of the composition in the sample chamber during the measurements. The sample volume was comparatively large $\frac{3}{4}$ mole of mixture) and the liquid nearly filled the entire sample chamber except for a capillary. This procedure kept the error due to vaporization very small.

After the data were taken, the composition of the 0.005- and 0.100-mole-fraction samples was checked to ensure that no leaks to the He^4 reservoir had occurred during the course of the measurements. The contents of the sample chamber were collected during warmup to room temperature, and a random sample analyzed with a CEC No. 621 mass spectrometer designed to do simple gas analysis. The results of this analysis were 0.005 and 0.1005 mole fractions, respectively. The resolution of the spectrometer was ± 0.0003 for the 0.005-mole-fraction mixture and ± 0.002 for the 0.100-mole-fraction mixture.[8]

Due to the presence of a capillary plug (which was noticed on filling the sample chamber), the composition of the 0.047-mole-fraction mixture had to be determined in an entirely different way. It was determined by comparing the absolute values of $\eta\rho_n$ with values determined in a previous experiment on a sample of slightly lower, but known composition. We estimate the uncertainty in composition of this mixture to be ± 0.001 mole fraction.

III. DETERMINATION OF NORMAL DENSITY OF MIXTURES

The physical quantity measured in the usual "viscosity" measurements of liquid helium is $\eta\rho_n$. In order to obtain η, it is necessary to have ρ_n. Measurements of ρ_n are quite difficult, but Dash and Taylor[3] showed that the normal density of He^3-He^4 mixture could be computed using the relation:

$$\rho_n(T^*, x_3) = \mathcal{O}_3\rho_3 + \frac{\mathcal{O}_4}{1+\gamma\mathcal{O}_3}\left[\rho_n(T^*, 0) + \gamma\mathcal{O}_3\rho_\lambda^0\right], \quad (1)$$

where $T^* = T/T_\lambda$ is the reduced temperature of the mixture; $\mathcal{O}_3$ the volume fraction of He^3 in the mixture equals $x_3(V_3/V_\lambda)$; $\mathcal{O}_4 = 1 - \mathcal{O}_3$; M_3 is molar mass of $He^3 = 3.01603$ on the C^{12} scale; $V_\lambda = x_3V_3 + x_4V_4$; V_3 is the partial molar volume of He^3 in the mixture which is 35.920×10^{-3} m^3/mole at $T = 2.0$ K; V_4 is the partial molar volume of He^4 in the mixture [here taken equal to the molar volume of He^4 at $T_\lambda(0) = 27.3870\times10^{-3}$ m^3 (Ref. 9)]; $\rho_3 = M_3/V_3 = 83.97$ kg/m^3; and $\gamma = 0.796$; ρ_λ^0 is the density of pure He^4 at $T_\lambda(0) = 146.2$ kg/m^3; $T_\lambda(0)$ is the accepted λ point of pure He^4 which is equal to 2.1720 K; $\rho_n(T^*, 0)$ is the normal density of liquid He^4 at a value of $T^*(0)$ equal to $T^*(x_3)$ of the mixture. Note that the experimental temperature corresponding to T^* in the term $\rho_n(T^*, 0)$ is $T_\lambda(0)T^* \neq T_\lambda(x_3)T^*$.

Subsequent to the publication of Ref. 3, improved measurements of several of the quantities used in the computation were made. To begin with, the value of V_3 used by Dash and Taylor was 35.552×10^{-3} m^3. This value was based on a value of 38.456×10^{-3} m^3 for the molar volume of pure He^3 at 2.0 K, a convenient temperature near T_λ of the mixtures. Subsequently, Kerr and Taylor[10] remeasured this quantity and obtained a value of 38.854×10^{-3} m^3. The value of V_3 has therefore been adjusted proportionately, and used in computing $\mathcal{O}_3$.

Using the same apparatus in which the improved measurements on He^3 were made, Kerr and Taylor[9] later measured the molar volume of He^4. It should be noted that we follow Dash and Taylor in using the value of the molar volume of pure He^4 at $T_\lambda(0)$ for V_4.

For dilute solutions of He^3, the term involving $\rho_n(T^*, 0)$ is the largest of the three terms contributing to $\rho_n(T^*, x_3)$. Clow and Reppy[11] showed that for $T_\lambda(0) - T < 0.06$ K, $\rho_s/\rho_4 = 1.438[T_\lambda(0) - T]^{2/3}$. Soon afterwards, Tyson and Douglass[12] determined the value of the exponent to be 0.666 ± 0.006. Therefore, the following expression was used to compute $\rho_n(T^*, 0)$ when $T^* < 1$:

$$\rho_n(T^*, 0) = \rho_4(T^*)\{1 - 1.438[T_\lambda(0) - T]^{0.666}\}.$$

Here, $\rho_4(T^*)$, the total density of liquid He^4 at T^*, has a maximum at $T^* = 1.00276$ and changes very little for $T^* > 1.00276$.[10] A small correction for the thermal expansion coefficient [~ 0.01 near $T_\lambda(0)$] has also been included, and the density of pure He^4 at $T_\lambda(0)$ has been taken as 146.2 kg/m^3.

In summary, then, the following equations were used to calculate ρ_n:

$$\rho_n(T^*, x_3) = \mathcal{O}_3\rho_3 + \frac{\mathcal{O}_4}{1+\gamma\mathcal{O}_3}\left[\rho_n(T^*, 0) + \gamma\mathcal{O}_3\rho_\lambda^0\right],$$

$$\mathcal{O}_3 = x_3/[x_3 + 0.76244(1 - x_3)],$$

$$\mathcal{O}_4 = 1 - \mathcal{O}_3, \quad \gamma = 0.796, \quad \rho_3(T^*) = 83.97,$$

$$\rho_n(T^*, 0) = 146.207[1 - 0.01\,T_\lambda(1.00276 - T^*)] \times [1 - 2.41175(1 - T^*)^{0.666}], \qquad T^* < 1$$

$$= 146.207[1 - 0.01\,T_\lambda(1.00276 - T^*)], \qquad 1 \leq T^* < 1.00276$$

$$= 146.207, \qquad T^* \geq 1.00276.$$

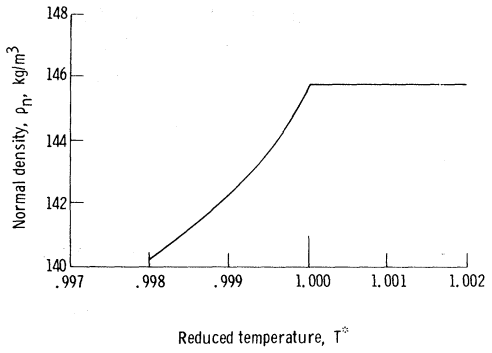

FIG. 3. Computed normal density vs T^* for $x_3 = 0.005$.

A graph of $\rho_n(T^*, \mathcal{O}_3)$ computed from this formula is shown in Fig. 3 for the 0.5% solution.

IV. RESULTS AND DISCUSSION

The measured values of $\eta\rho_n$ versus T for the three He^3-He^4 mixtures and for pure He^4 are shown in Fig. 4. The results show clearly that $\eta\rho_n$ is a monotonic decreasing function of He^3 concentration. Although this behavior is to be expected qualitatively since the addition of He^3 decreases the density of the mixture, the viscosity itself decreases monotonically with He^3 concentration at any fixed value of $T - T_\lambda(x_3)$ within the range of temperature and composition considered in this investigation (see Fig. 6).

The functional dependence on T of all the $\eta\rho_n$ curves seems to be qualitatively similar, so some quantitative measure of the similarity among different concentrations would be of interest. As was indicated in the Introduction, doubly reduced plots provide such a measure. A doubly reduced plot is one on which both the ordinate and the abscissa are expressed in multiples of the respective values of the unreduced quantity at $T_\lambda(x_3)$. It should be noted that, on such a plot, the transition between the normal and the superfluid state is at the location (1, 1) for all concentrations. A superscript * is used to distinguish a reduced quantity from the corresponding unreduced one.

A plot of $(\eta\rho_n)^*$ versus T^* is shown in Fig. 5(a) for pure He^4, for a mixture containing $\frac{1}{2}\%$ He^3 and for another mixture containing 10% He^3. Data for the 4.7% mixture are not included because they fall very close to the 10% data and would make it more difficult to discern the change in the curves as a function of concentration. On this plot, the curves are indeed very similar for all the mixtures. However, there is a clear tendency for the curves to rotate clockwise about the (1, 1) point with increasing x_3 up to ~0.05.

An expanded and smoothed $(\eta\rho_n)^*$-versus-T^* plot is shown in Fig. 5(b) for the $\frac{1}{2}\%$ mixture. The experimental λ point for the $\frac{1}{2}\%$ curve could be determined to less than ± 0.1 mK. (Of course, this is not the accuracy.) The absolute temperature of the measurements is known only to within 2.0 mK. Similarly, the precision of the values of $(\eta\rho_n)$ is ~0.05%, whereas the accuracy was not determined.

The precision of the results for the mixtures is clearly very much better than for pure He^4 [see Fig. 5(a)]. In particular, it was possible to determine $T_\lambda(x_3)$ from expanded Fig. 4 curves with

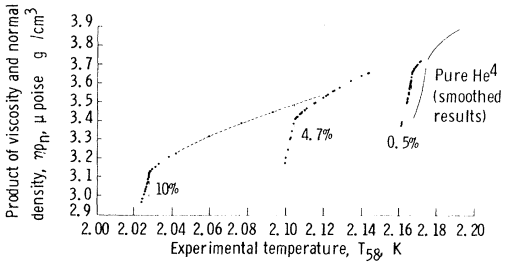

FIG. 4. Product of viscosity and normal density as function of experimental temperature for pure He^4 and dilute He^3-He^4 mixtures. (Precision in T_{58} is better than ± 0.1 mK; the absolute T_{58} is uncertain within ± 2 mK; precision in $\eta\rho_n$ is about 0.05%. The approximate T_{58} absolute temperature may be obtained by subtracting 1.7 mK from experimentally determined temperatures shown on abscissa.)

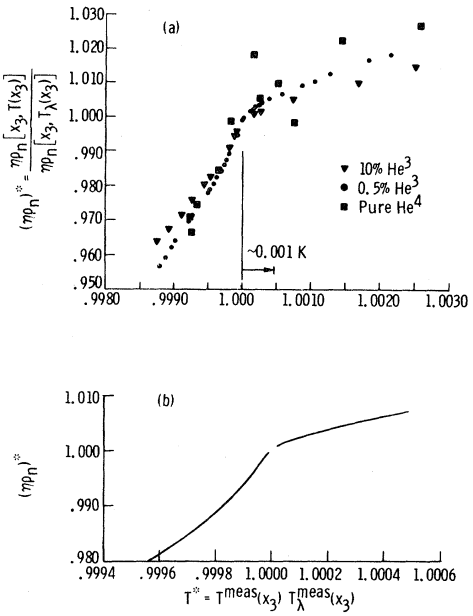

FIG. 5. Reduced product of viscosity and normal density as function of reduced temperature. (a) Wide range; (b) expanded and smoothed plot for 0.5%-He^3 mixture.

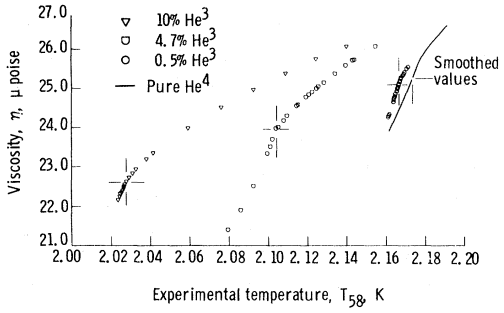

FIG. 6. Viscosity as a function of experimental temperature for pure He^4 and dilute He^3-He^4 mixtures.

reasonable confidence when x_3 was nonzero. Therefore, the values of $T_\lambda(x_3)$ which were used to analyze the data and to determine $T^*(x_3)$ were obtained from such curves. This procedure was clearly unsatisfactory for pure He^4, so that $T_\lambda(0)$ was obtained by extrapolating the value of $T_\lambda(0.005)$ to zero concentration of He^3. The determination of $T_\lambda(x_3)$ and $T_\lambda(0)$ was described in Sec. II.

For the mixtures, the values of $(\eta\rho_n)$ at the λ point $(\eta\rho_n)_\lambda$ were determined from smoothed expanded plots of the curves in Fig. 4 by noting the ordinates corresponding to the values of $T_\lambda(x_3)$. It was decided, that for pure He^4, a better estimate of $(\eta\rho_n)_\lambda$ could be obtained by plotting x_3 against the $(\eta\rho_n)_\lambda$'s for the mixtures and extrapolating to zero He^3 concentration.

It should be noted that these procedures yield only the experimental values of $(\eta\rho_n)_\lambda$ and $T_\lambda(x_3)$. However, these quantities are the ones which are relevant for comparing results among different concentrations, since the "true" absolute values were not determined.

The absolute values of $(\eta\rho_n)$ in the present experiment appear to be about 0.14 $\mu P g cm^{-3}$ too high (about 4% too high at T_λ for pure He^4) compared to the values reported in Refs. 5 and 6 which are probably more reliable. (A comparison at lower temperatures leads us to believe that the crystal was slightly cocked in the present experiment.) With regard to the temperature, we conclude that approximate values of temperature on the T_{58} scale can be obtained by subtracting 1.7 mK from the experimental temperatures on the abscissas of Figs. 4 and 6.

It has also been possible to use the present results to correct the absolute temperature on the T_{58} scale shown in Table I of Refs. 5 and 6. The correction is based on a finding that the pure-He^4 data from these earlier measurements can best be made consistent with the present data if the λ point in these references is moved from the high-temperature side of the data gap to the low-temperature side. In these references the location of the λ point of pure He^4 was somewhat uncertain due to the absence of data over a 2-mK inverval which included $T_\lambda(0)$. The λ point was taken to be near the high-temperature side of the data gap partly because this side of the data gap corresponded to a measured experimental temperature of 2.172 K. The present investigation has demonstrated that our experimental temperature could not be used to determine the λ point of pure He^4 more accurately than within a few mK. Thus, the aforementioned λ point in Refs. 5 and 6 could actually have been anywhere within the data gap, and some other factors would have to be considered in deciding where the λ point lay.

A doubly reduced plot of the pure-He^4 data from Ref. 5 was made and compared with the data from the present investigation. It was found that the two plots could be made nearly identical if the λ point in Ref. 5 were moved from the higher-temperature side of the data gap to the lower-temperature side. We have, therefore, concluded that the results of Ref. 5 should be corrected. This correction requires that 1.4 mK must be added to all temperatures listed in Table I of Refs. 5 and 6. With this correction, the temperature values listed in the table are the absolute temperatures on the T_{58} scale with $T_\lambda(0)$ at 2.172 K.

The viscosity of the mixtures was also of interest. This quantity was derived from the $\eta\rho_n$ values by using the calculated values of ρ_η. The variation of ρ_η with $T(x_3)$ is so great near $T_\lambda(x_3)$ that serious errors in η could result from small errors in the absolute temperature. Therefore, ρ_n was computed as a function of $T^*(x_3)$, which we know much better than $T(x_3)$ absolute. Figure 6 shows η versus $T(x_3)$ for pure He^4 and for three mixtures. The results show that, as was mentioned earlier, η decreases with x_3 at a given value of $T - T_\lambda$.

The reader should note that this conclusion is not meant to be extrapolated for $T(x_3) < T_\lambda(x_3)$, to values of $T(x_3) - T_\lambda(x_3)$ larger than those shown in Fig. 6. In addition, it should be kept in mind that the computation of $\rho_n(T^*, x_3)$ cannot be reliably extrapolated to values of T^* and x_3 outside of the range used here.

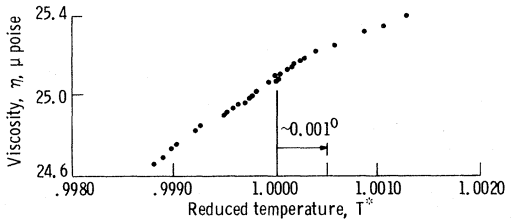

FIG. 7. η vs T^* for $x_3 = 0.005$.

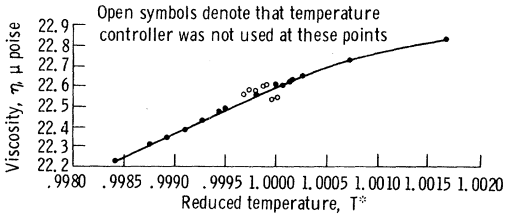

FIG. 8. η vs T^* for $x_3 = 0.100$.

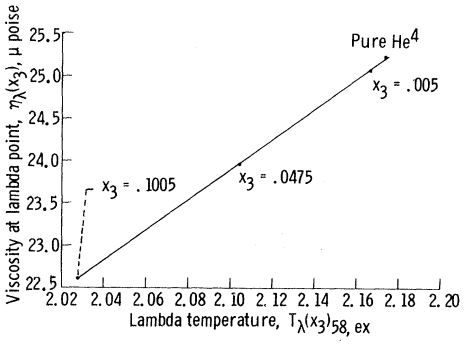

FIG. 9. Viscosity at λ point as function of λ temperature for pure He^4 and three He^3-He^4 mixtures. [The straight line was drawn through points corresponding to $x_3 = 0.005$ and $x_3 = 0.1005$ (the most reliable points). For pure He^4, $T_\lambda(0)$ was obtained by adding a correction to $T_\lambda(0.005)$; $\eta_\lambda(0)$ was obtained as follows: First, a plot of $\eta\rho_n$ against x_3 was extrapolated to zero He^3 concentration; then, this value was divided by the accepted value of ρ_n at $T_\lambda(0)$, which is 146.2 kg/m^3.]

Figure 7 is an expanded plot of η versus T^* for $x_3 = 0.005$. This curve shows that neither η nor $d\eta/dT$ is discontinuous across $T_\lambda(x_3)$. The conclusion to be drawn from this figure is that the sharp changes in $\eta\rho_n$ across T_λ are due entirely to ρ_n. Figure 8 shows, in a less precise manner, that this is also true for the 0.100 mole fraction.

The significance of the apparent slight change in slope of η versus T^* at a temperature about 1 mK above the λ point is not clear. However, as can be seen from Fig. 5(b) and from an expanded plot of the $\frac{1}{2}\%$ curve in Fig. 4 (not shown), it can be stated with confidence that this break in the slope of the η-versus-T^* curve cannot be due to an improperly determined λ point.

Another point worth noting is shown in Fig. 9. Let $\eta_\lambda(x_3)$ denote the viscosity at $T_\lambda(x_3)$ for a He^3 concentration given by x_3. Then Fig. 9 shows that the dependence of $\eta_\lambda(x_3)$ on $T_\lambda(x_3)$ is well fitted by a straight line. This result does not seem to have been published before now. It has been mentioned earlier that $T_\lambda(x_3)$ is closely approximated by $(1 - x_3)^{2/3} T_\lambda(0)$ (Ref. 3). Therefore, it may be concluded from Fig. 9 that

$$\eta_\lambda(x_3) - \eta_\lambda(0) = A(1 - x_4^{2/3}) T_\lambda(0),$$

where A is a constant equal to the negative of the slope of the line in Fig. 9.

Finally, we wish to set forth our reasons for believing that η and $d\eta/dT$ of pure He^4 are continuous across $T_\lambda(0)$. Of course, the obvious points that η and $d\eta/dT$ are very smooth across $T_\lambda(x_3)$ for the $\frac{1}{2}\%$ mixture and that $\frac{1}{2}\%$ is only a small amount of He^3, are important parts of the argument. However, the case is somewhat stronger than this. First of all, the value of $T_\lambda(0)$ was obtained by adjusting $T_\lambda(x_3)$ to zero concentration of He^3 and $(\eta\rho_n)_\lambda$ was obtained by extrapolating the $(\eta\rho_n)$ curve for the mixtures, as explained previously. The doubly reduced plots of $(\eta\rho_n)$ versus T for pure He^4 using these values blend smoothly into the curves for the mixtures [taking into consideration the comparatively poor precision of the He^4 data near $T_\lambda(0)$]. The same behavior is evident for the 10% solution as shown in Fig. 8. Second, there does not seem to be any tendency for η to become ill behaved as x_3 decreases. The normal density, of course, does have a discontinuous slope at $T_\lambda(x_3)$. We feel that, taken together, these facts indicate strongly that η and $d\eta/dT$ are both likely to be continuous across $T_\lambda(0)$.

Note added in manuscript. After this manuscript was submitted, it was called to our attention[13] that our data for $x_3 = 0.005$ are consistent with the existence of a weak discontinuity of the form $1 - \eta^* = A(1 - T^*)^\alpha$, where $\alpha < 1$. An examination of Fig. 7 shows that if such a discontinuity in $d\eta/dT$ exists, it is so small that an order-of-magnitude increase in experimental precision would be required to see it on a plot of η vs. T.

---

[1]J. M. Reynolds, R. G. Hussey, D. P. Thibodeaux, B. E. Tucker, and J. Urrechaga-Altuna, Louisiana State University Report Nos. AFASD-TDR-817, Pt. 1 and DDC AD-428267, 1963 (unpublished).

[2]B. Welber, Phys. Rev. 119, 1816 (1960).

[3]J. G. Dash and R. D. Taylor, Phys. Rev. 107, 1228 (1957).

[4]F. A. Staas, K. W. Taconis, and K. Fokkens, Physica 26, 669 (1960).

[5]R. W. H. Webeler and D. C. Hammer, NASA Report No. TND-4381, 1968 (unpublished).

[6]R. W. H. Webeler and D. C. Hammer, Phys. Letters 15, 233 (1965).

[7]B. Welber and S. L. Quimby, Phys. Rev. 107, 645 (1957).

[8]Thanks are due D. Otterson who kindly performed the analysis.

[9]E. C. Kerr and R. D. Taylor, Ann. Phys. 26, 292

(1964).
[10]E. C. Kerr and R. D. Taylor, Ann. Phys. 20, 450 (1962).
[11]J. R. Clow and J. D. Reppy, Phys. Rev. Letters 16, 887 (1966).
[12]J. A. Tyson and D. H. Douglass, Jr., Phys. Rev. Letters 17, 472 (1966).
[13]Guenter Ahlers (private communication).

PHYSICAL REVIEW A VOLUME 5, NUMBER 4 APRIL 1972

Resonant Multiphoton Excitations by Strong Driving Fields

B. R. Mollow
Department of Physics, The University of Massachusetts, Boston, Massachusetts 02116
(Received 7 September 1971)

Multiphoton transitions are discussed for the case of a resonant driving field strong enough to produce saturation. The atomic system is described in general terms, and the possibility of inversion asymmetry is allowed. The equations of motion for the density submatrix referring to the pair of resonantly coupled states are found by expanding the full atomic density operator in harmonics of the field frequency, and then systematically reducing the equations of motion which result. The effective n-photon coupling parameter and the shift in resonance frequency emerge naturally from this reduction.

In this paper we shall consider the problem of an atom driven by an external field which induces transitions between a particular pair of atomic states by means of an n-photon excitation process.[1-3] The field will be allowed to be strong enough and near enough to resonance to cause appreciable saturation, and hence it will be necessary to describe the state of the system in terms of a density operator which may have large off-diagonal components. We shall develop the analysis in a systematic way, by expressing the density operator in terms of a suitable expansion in field harmonics, and identifying large and small terms. The equations of motion for the 2×2 submatrix referring to the pair of resonantly coupled states then emerge directly from a straightforward reduction of the equations of motion for the full atomic density matrix.

Let us consider a general atom with energy eigenstates $|j\rangle$ and corresponding eignevalues E_j, driven by the electric field

$$\vec{\mathbf{E}}(t)=(1/\sqrt{2})\,\hat{e}_0\,[\mathcal{E}(t)+\mathcal{E}^*(t)]\,, \tag{1a}$$

where

$$\mathcal{E}(t)=\mathcal{E}_0\,e^{-i\omega t}\,. \tag{1b}$$

We introduce the quantities

$$\omega_{jk}\equiv(E_j-E_k)/\hbar\,, \tag{2a}$$

$$\lambda\equiv(\vec{\mu}\cdot\hat{e}_0)/\hbar\sqrt{2}\,, \tag{2b}$$

where $\vec{\mu}$ is the dipole-moment operator, which, in order to allow for the possibility of inversion nonsymmetric cases,[4,5] may be allowed to have diagonal as well as off-diagonal matrix elements. The equations of motion for the atomic density matrix in the case of collisional relaxation[6] are then

$$\left(\frac{d}{dt}+i\omega_{jk}+\kappa\right)\sigma_{jk}(t)-\kappa\,\delta_{jk}\bar{n}_j^{(0)} =i(\mathcal{E}(t)+\mathcal{E}^*(t))[\lambda,\ \rho(t)\,]_{jk}\,, \tag{3}$$

where κ is the mean collision frequency, and $\bar{n}_j^{(0)}$ is the mean thermal occupation number for the state $|j\rangle$.

We wish to consider the case in which the field induces resonant transitions between a particular pair of states, $|0\rangle$ and $|1\rangle$, by means of an n-photon absorption process, i.e.,

$$\omega_{10}\approx n\omega. \tag{4}$$

We shall assume that no other pair of states is similarly coupled (for any value of n) by the driving field. In that case the time-dependent density operator may be expanded in a harmonic series in the field frequency ω, where the large components are the slowly varying diagonal terms $\bar{n}_j(t)$ and the off-diagonal terms oscillating at the frequency $\pm n\omega$, and where the terms oscillating at the other harmonic frequencies may be assumed small. The density operator thus has the expansion

$$\rho(t)=\bar{n}(t)+(\alpha(t)+\alpha^\dagger(t))+\sum_{\gamma=1(\gamma\neq n)}^{\infty}(\beta^{(\gamma)}(t)+\beta^{(\gamma)\dagger}(t))\,, \tag{5}$$

where the time dependence of $\alpha(t)$ and $\beta^{(\gamma)}(t)$ is

$$\alpha(t)\sim e^{-in\omega t} \tag{6a}$$

and

$$\beta^{(\gamma)}(t)\sim e^{-i\gamma\omega t}\quad\text{for }\gamma=1,\ldots,n-1,\ n+1,\ldots\,. \tag{6b}$$

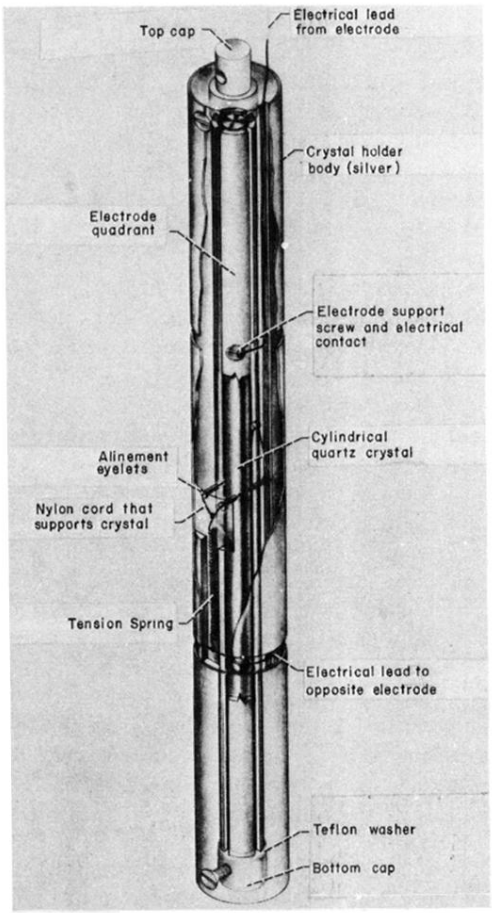

FIG. 1. Torsional crystal suspension system prior to placement in sample chamber of Fig. 2.